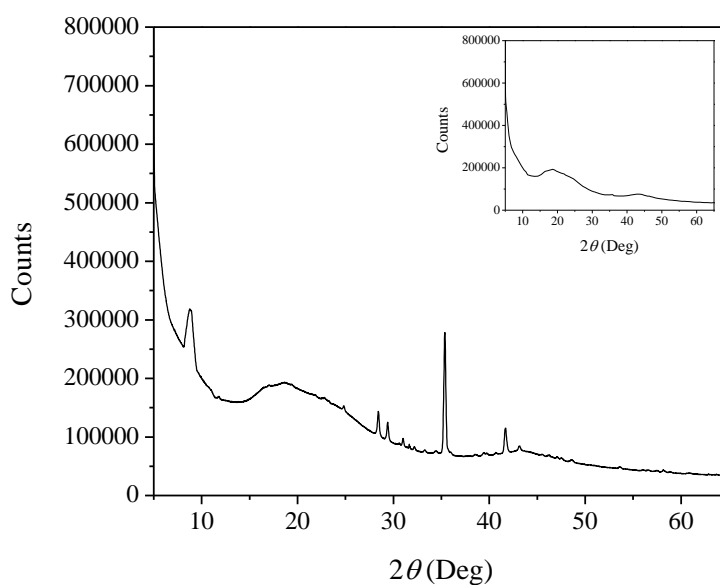


**“Electrochemical Deposition of Hierarchical Micro/Nanostructures of Copper Hydroxysulfates  
on Polypyrrole-Polystyrene Sulfonate Films”**

by Andreoli E. *et al.*

The copper-based micro/nanostructures were characterized using XRD. In order to identify the crystalline components of the copper-based structures, the XRD patterns of the bare and copper-modified electrodes were analyzed and compared. The XRD pattern of a glassy carbon (GC) bare electrode is shown in Figure 1.



**Figure 1.** XRD pattern of a bare glassy carbon electrode used for the electrodeposition of hierarchical copper-based micro/nanostructures. The inset shows the background trace of the pattern.

The two broad signals at about 20.0° and 44.0° are characteristic of the background trace of GC, as reported in the literature.<sup>1</sup> To facilitate the identification of the smaller peaks; the background trace was subtracted from the raw data to obtain the pattern in Figure 2.

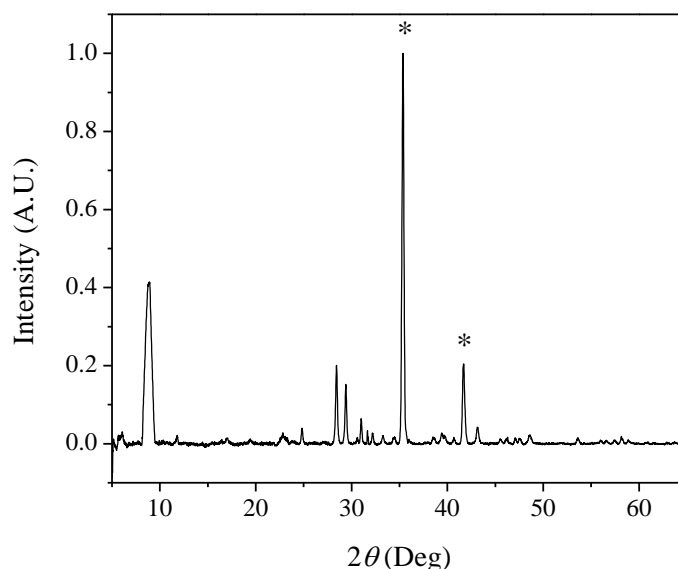


**Figure 2.** XRD pattern of a bare glassy carbon electrode obtained from the subtraction of the raw pattern and background trace given in Figure 1. The labeled peaks (\*) were identified as due to the silver loaded-resin used for the electrical contact between glassy carbon rod and copper wire.

The sharp peaks at  $35.3^\circ$  and  $41.7^\circ$  are due to the presence of Ag from the silver-loaded resin used to assemble the electrode (The working electrode was prepared from a rod of high purity glassy carbon, 99.99+ %. A piece of rod of about half centimeter was cut and set in a PVC holder with epoxy resin. The electrical contact was made with a copper wire attached at one end of the piece with highly conducting silver-loaded resin). These peaks appear down-shifted compared to those found in the literature<sup>2</sup> at  $38.1^\circ$  and  $44.3^\circ$  for Ag, because the silver contact was placed about 5 mm below the surface of analysis (*i.e.*, the electrode surface). The origin of the other peaks is unknown, but they are likely to be related to the presence of crystalline fillers in the electrode mount made of PVC.

It is known that nanothin films of PPy form ordered arrays of helical PPy-doped macromolecules organized in micro-islands.<sup>3,4</sup> The XRD of PPy-Tosylate film reported in the literature<sup>5</sup> shows the presence of one broad diffraction peak at about  $25^\circ$ . The actual position of the peak is dependent on the dopant. The XRD of the PPy-PSS film has not been reported. However, the small amount of polymer

and the sub-micrometer size of the crystallites in the PPy-PSS film<sup>3</sup> should only give a weak broad peak. The XRD pattern of the copper-based structures deposited on PPy-PSS is given in Figure 3.

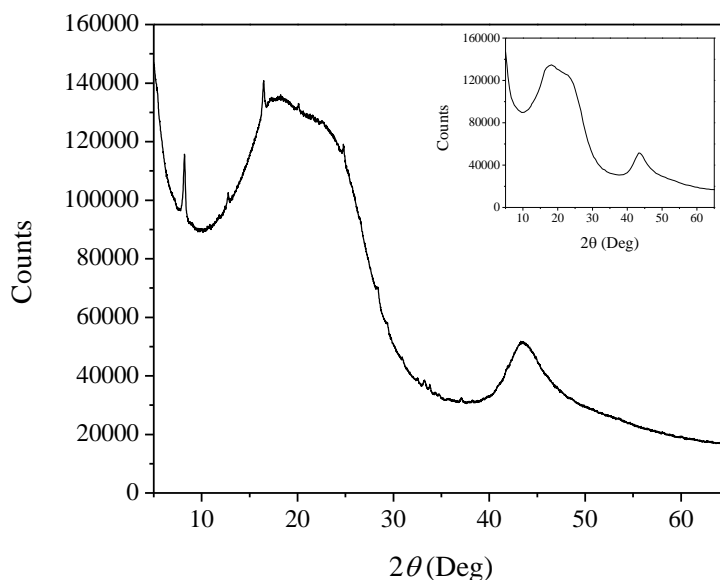


**Figure 3.** XRD pattern of the hierarchical copper-based micro/nanostructures electrodeposited on 120 nm PPy-PSS film from oxygen saturated 0.10 M CuSO<sub>4</sub> at 0.10 V vs. SCE. The electrode material was glassy carbon and the copper was deposited to a charge of 0.2 C/cm<sup>2</sup>. In the inset, the background trace that was subtracted from the raw pattern to obtain the pattern shown in Figure 5.

Clearly, the background trace is dominated by the two signals of GC.<sup>1</sup> The smaller and sharper peaks are enlarged in Figure 4. On subtracting the background trace several diffraction peaks are evident, as shown in Figure 5. This pattern is compared to that obtained with the GC substrate in Figure 6. In the pattern of the copper-based structures the Ag peaks of the substrate are absent since copper absorbs the X-rays and limits their penetration into the electrode. Also, the position and shape of the peak at 8.2° is different compared to the one at 8.9° of the substrate, as shown in the inset. However, the peaks at 28.4° and 29.4° correspond well in the two patterns.

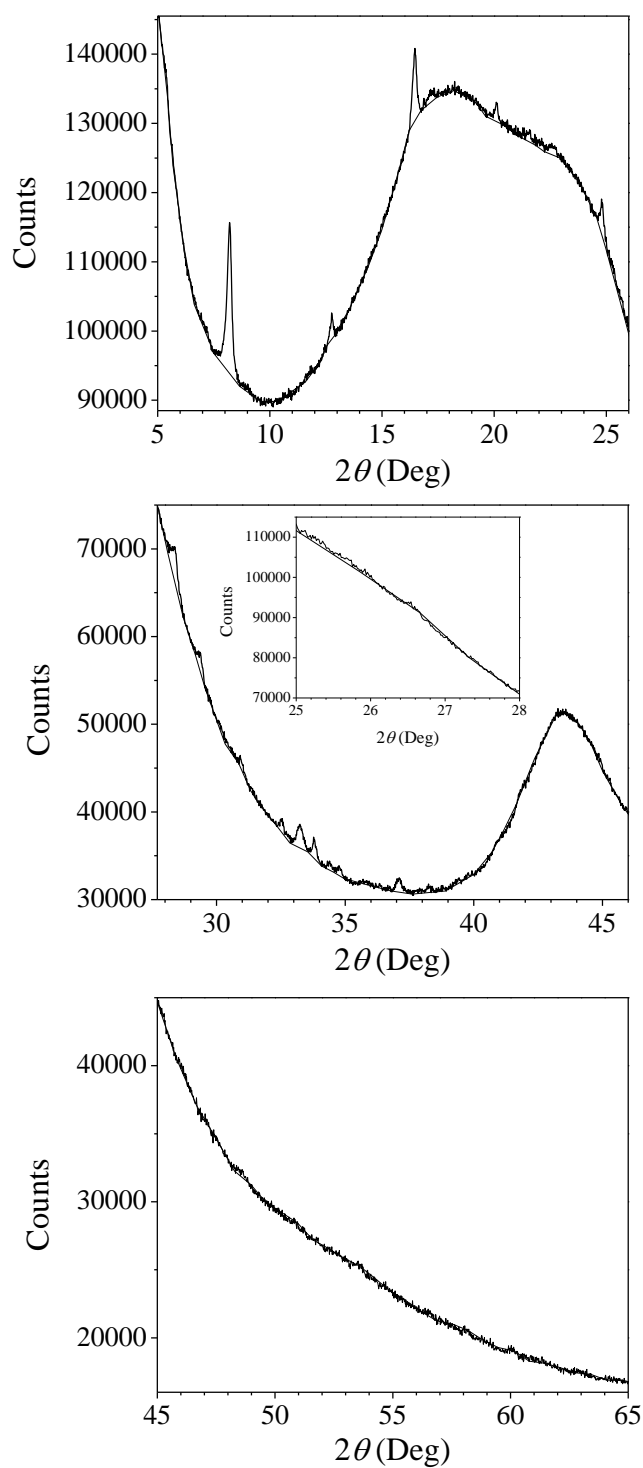


**Figure 4.** Enlargements of the XRD raw and background superimposed patterns of the hierarchical copper-based micro/nanostructures shown in Figure 3. Small diffraction peaks are visible in the portions of the raw pattern emerging above the background trace. The subtraction of the background pattern from the raw pattern allows the clear identification of the diffraction peaks due to the copper-based micro/nanostructures, as shown in Figure 5.

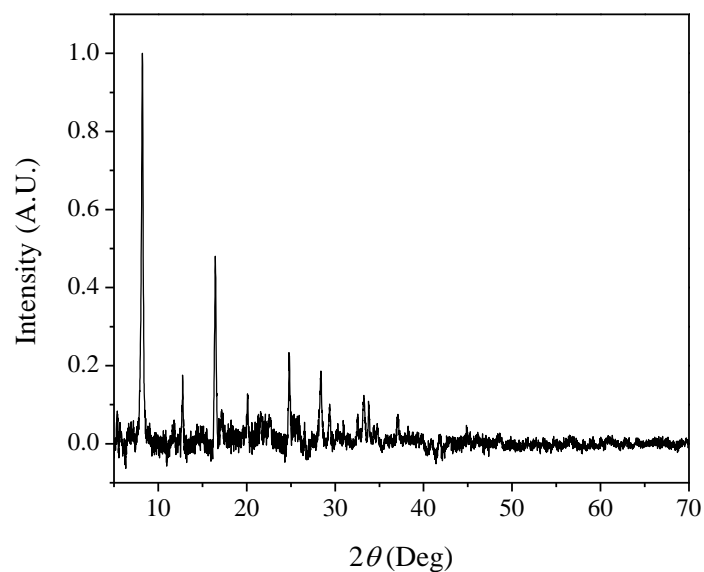


**Figure 5.** XRD pattern of the hierarchical copper-based micro/nanostructures obtained from the subtraction of the background traces from the raw pattern which are given in Figure 3.

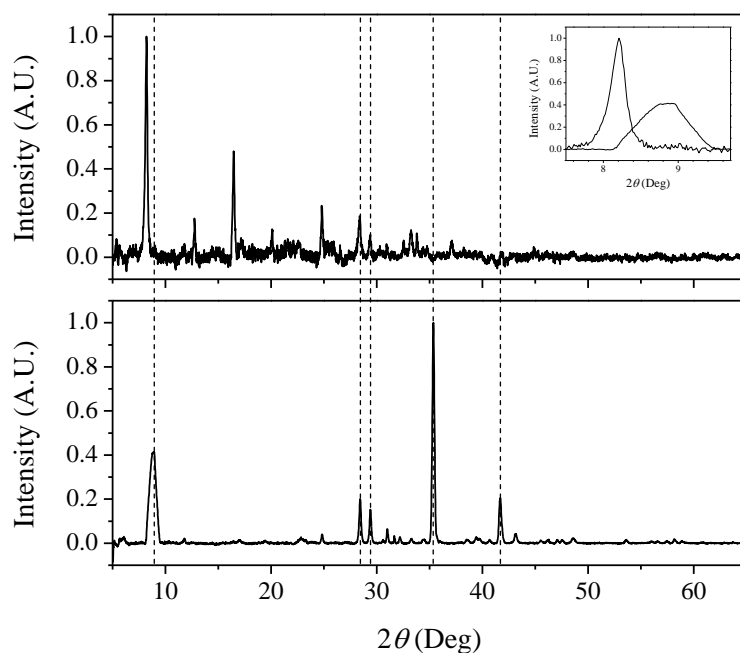


**Figure 6.** Comparison of the XRD patterns of hierarchical copper-based micro/nanostructures (top) and bare glassy carbon electrode (bottom). The inset shows the superimposition of the peaks of the two patterns in the low diffraction angle region. The dashed lines indicate the position of the main peaks of the bare GC electrode.

The assignment of the XRD peaks of the hierarchical copper-based micro/nanostructures is reported in the manuscript and also here for completeness (Figure 7 and Table 1). It is evident that the majority of the peaks is related to the presence of copper sulfate hydroxide hydrate,  $[\text{CuSO}_4]_2[\text{Cu}(\text{OH})_2]_3 \cdot 5\text{H}_2\text{O}$ . An additional crystalline phase is identified as posnjakite,  $\text{CuSO}_4[\text{Cu}(\text{OH})_2]_3 \cdot \text{H}_2\text{O}$ .

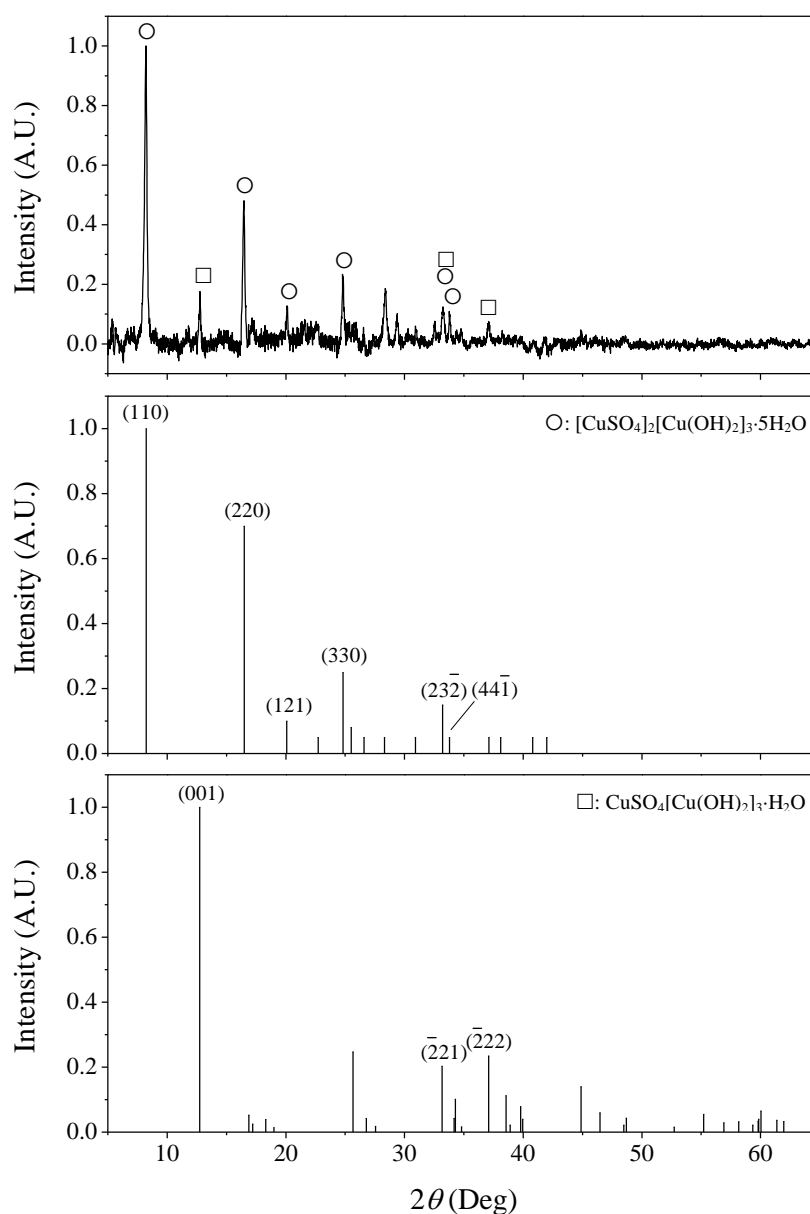


**Figure 7.** XRD peak assignment for the hierarchical copper-based micro/nanostructures. The diffraction peaks were identified as those of copper sulfate hydroxide hydrate (○) and posnjakite (□). The corresponding Miller indexes, (*hkl*), are given for each of the assigned peaks.

**Table 1. Comparison of the XRD peaks of experimental hierarchical copper-based micro/nanostructures and reference compounds.**

Experimental		References			
Position (°2θ)	Intensity (A.U.)	[CuSO <sub>4</sub> ] <sub>2</sub> [Cu(OH) <sub>2</sub> ] <sub>3</sub> ·5H <sub>2</sub> O		CuSO <sub>4</sub> [Cu(OH) <sub>2</sub> ] <sub>3</sub> ·H <sub>2</sub> O	
		Position (°2θ)	Intensity (A.U.)	Position (°2θ)	Intensity (A.U.)
8.209	1.00	8.241	1.00	–	–
12.754	0.18	–	–	12.750	1.00
16.464	0.48	16.494	0.70	–	–
20.091	0.13	20.073	0.10	–	–
24.786	0.23	24.816	0.25	–	–
33.242	0.12	33.216	0.15	33.160	0.20
33.777	0.11	33.797	0.05	–	–
37.103	0.07	37.121	0.05	37.100	0.23

## REFERENCES

- (1) Noda, T.; Inagaki, M. *Bull. Chem. Soc. Jpn.* **1964**, *37*, 1534-1538.
- (2) Suh, I. K.; Ohta, H.; Waseda, Y. *J. Mater. Sci.* **1988**, *23*, 757-760.
- (3) Yang, R.; Naoi, K.; Evans, D. F.; Smyrl, W. H.; Hendrickson, W.A. *Langmuir*, **1991**, *7*, 556-558.
- (4) Yang, R.; Evans, D. F.; Christensen, L.; Hendrickson, W. A. *J. Phys. Chem.* **1990**, *94*, 6117-6122.
- (5) Buckley, L. J.; Roylance, D. K.; Wnek, G. E. *J. Polym. Sci. Pt. B-Polym. Phys.* **1987**, *25*, 2179-2188.